

and Binding Properties of the Oxoglutarate Translocator Heart Mitochondria

Claire DUYCKAERTS, Claude LIÉBECQ

Assistance of Laurette Bertrand and Eli Dethier

Chimie et de Physiologie Générales, Institut Supérieur d'Education Physique de l'Université de Liège

LUSE-GOFFART

Chimie Générale et de Chimie Physique, Institut de Chimie de l'Université de Liège

16, 1978/July 4, 1979)

The kinetic study of the oxoglutarate_{out}/malate_{in} exchange through the inner mitochondrial membrane of rat-heart mitochondria has been completed and extended to higher external-oxoglutarate and to lower internal-malate concentrations. It has been found that the external-oxoglutarate inhibits the exchange at high concentration. This excess-substrate inhibition is preceded by a sharp increase in the initial rate. The kinetic-saturation curve by the internal malate presents an apparent positive cooperativity that may be interpreted in different ways. The independence of the effects of the external-oxoglutarate on the initial rate has been observed again and supports the conclusions reached in our previous work.

A method for the determination of oxoglutarate binding to the external face of the inner mitochondrial membrane is described. The binding curve shows four intermediary plateau regions that reflect significant apparent K -effects, alternatively negative and positive.

For external-oxoglutarate concentrations below the region of excess-substrate inhibition, the binding-saturation curve and the kinetic-saturation curve are similar, demonstrating that K -effect is predominant. A particularly wide intermediary plateau that seems to correspond to the saturation of the active sites is common to both saturation curves. A clear lack of proportionality between the two curves at low oxoglutarate concentrations seems to indicate that more than one catalytic-rate constant is implied in the exchange kinetics.

Two models of the oxoglutarate carrier are presented. Both lead to a minimum degree of 10% of the equation of the binding of oxoglutarate to the catalytic sites. In the first model this corresponds to subunits associated into a single oligomer while in the second model this results from a mixture of monomeric, dimeric, trimeric and tetrameric associations.

Translocators embedded in the inner mitochondrial membrane catalyses exchange-diffusion between the intramitochondrial and the extramitochondrial compartments following a one-to-one stoichiometry. These translocators show a specificity for the anions exchanged and a sensitivity to inhibitors (for a review, see [1]) in various metabolic processes occurring inside the mitochondrial matrix.

The transport is subordinated to the properties of the substrates and to the kinetic characteristics of the reactions they take part in; in this way they may have a regulatory rôle in cellular metabolism. For example, the oxoglutarate translocator is involved in the transport of reducing equivalents across the inner mitochondrial membrane of

mitochondria via the malate-aspartate shuttle and thus control both internal and external NADH/NAD⁺ ratios. To conceive valid experiments aimed at testing such a rôle, the detailed kinetics and the mode of action of the translocator *in situ* must be known first.

The translocator catalyses various one-to-one exchanges, internal against external substrate; the initial concentration of both substrates influences the initial rate in a way depending on the mechanism and on the kinetic characteristics. These can be elucidated if the characteristics of the various permissible exchanges and of the products of inhibition are determined. We have measured the initial rates of exchanges, in spite of technical difficulties, because their interpretation is easier. For the best metabolic interpretation, kinetic studies of oxoglutarate translocation should be done at physi-

logical temperature. However, the initial-rate period (between initial transient phase and product-inhibited rate), if still present at such a temperature will be extremely short; it is not yet accessible experimentally. Thus our experiments have been done at 2 °C.

Dicarboxylates (except oxoglutarate) can be translocated by several translocators [1]; for example malate may be translocated by the dicarboxylate, tricarboxylate and oxoglutarate translocators. To avoid composite data, it is necessary to be sure that one translocator species only is implied in the initial rate measurement when dicarboxylate/dicarboxylate exchange is measured. We have demonstrated [2] that the tricarboxylate carrier is inactive in heart mitochondria under our experimental conditions and that the dicarboxylate carrier can be inhibited by mersalyl at a concentration that does not affect the oxoglutarate carrier, the latter being defined as the only 'system' which can translocate oxoglutarate.

Centrifugation was used to interrupt the exchanges in our first set of experiments [3–5]. The initial rates of 12 different exchange reactions showed Michaelian behaviour and led to the conclusion that the translocator follows a sequential mechanism [5a], the so-called 'rapid-equilibrium random bi-bi' mechanism, and therefore possesses two binding sites (one internal and one external) for the substrates, the transport being achieved, after two local and independent configuration changes, by a simultaneous displacement of the two anions, this displacement being the limiting step of the exchange reaction. The rate equation is the product of two one-substrate functions implying independence between the internal and the external sites: the K_m of each substrate is independent of the concentration of the other substrate. Evidence for a sequential mechanism with translocation as the rate-limiting step has also been reported recently for the aspartate-glutamate exchange [6]. New data suggest the same behaviour for the adenine nucleotide translocator [7] and for the acylcarnitine-carnitine exchange [8].

The centrifugation-stop technique blocked the exchange within 26 s. This long quenching time, part of the incubation time, restricts the substrate-concentration-dependence study to a limited range of rather low external-substrate concentrations because product inhibition occurs very soon at higher concentrations and substrate depletion at lower concentrations.

An inhibitor-stop technique [9] made it possible to reduce the incubation time because instantaneous quenching of the exchange reaction occurs after addition of the inhibitor, phenylsuccinate. Exchanges at higher and lower external-oxoglutarate concentrations with 4-mM internal malate could thus be measured [10].

This extended kinetic study confirmed the conclusions of the previous work but led to a saturation

curve v_0 versus external-oxoglutarate concentration presenting two intermediary plateaus, i.e. apparent alternating cooperativities.

Non-Michaelian transport kinetics are not a surprising phenomenon, as stressed by Kotyk who discussed five causes of non-linearity of reciprocal plots [11]. Evidence for apparent alternating cooperativities is indeed found for calcium transport in liver mitochondria [12]. The occurrence of intermediary plateau region(s) is well known in enzyme kinetics and has received various interpretations [13–20].

Taking into account the fact that the rate equation of the oxoglutarate carrier is the product of two one-substrate functions, two interpretations may be considered in our case [10].

a) The translocator possesses several external binding sites (probably at least five) whose progressive saturation by oxoglutarate leads to alternate negative and positive cooperativity [13].

b) Several translocator species participate in the exchange reaction. For example, the kinetic saturation curve could be the sum of the contributions from three translocators with quite different half-saturation concentrations, one possessing hyperbolic kinetics and the other two, sigmoidal kinetics. Cooperativity between external sites is still present in the two latter species but alternating cooperativities are no longer required. However, the individual rate equations of the different species must have a common part [10], either the external or the internal-substrate function so that the different translocators may differ only (as regards their kinetic parameters) by their external or by their internal moiety. This important restriction makes the occurrence of several species rather less likely.

In any case the mechanism is rapid-equilibrium random bi-bi with external-site interactions, while the internal sites do not interact with the external sites. On one side of the membrane at least, the binding sites are identical when none of them is loaded. The translocator could be made of a symmetrical association of identical subunits, each bearing a pair of binding sites (one internal and one external) with subunit interactions at the outer side of the membrane. The exchange would require two independent local changes of configuration induced by the binding of the substrates to one subunit.

Less extensive data were available concerning the internal sites, except the apparent Michaelis-Menten behaviour in the limited range of concentrations used [3–5, 10]. The kinetic-saturation curve will be described for an extended scale of internal-malate concentrations made possible by a progressive unloading of the internal malate of the mitochondria. As will be shown the kinetics are no longer strictly hyperbolic.

We also provide additional data relative to the external-substrate dependence: (a) additional rate-

measurements at low concentrations, (b) extension of the curve to very high concentrations showing excess-substrate inhibition, (c) demonstration of the independence of the binding of the two substrates over the full range of external-oxoglutarate concentrations at three internal-malate concentrations.

The initial-rate study has shown a complex dependence on external-substrate concentration. The observed cooperativities in the kinetic curve are due, at least in part, to external-site interactions which may act either at the level of substrate binding (*K*-effects) and/or at the level of the catalytic rate constants of the active complexes (*V*-effects, see [21] § 7.3.4., pp. 137–140). To choose between these possibilities, two approaches are possible: calculate all the parameters of the initial-rate equation or study the binding of the external substrate. The first approach is impracticable because the rate equation is the ratio of two polynomials of unknown and high degree, and the number of parameters involved is large for the number of experimental points. After numerous unsatisfactory attempts of computation, the binding of external substrate was measured in whole mitochondria thus leaving the translocator in its natural environment.

This was done at 2 °C for oxoglutarate concentrations ranging from 0.1 to 230 μM. The translocation of oxoglutarate into the matrix space was kept as low as possible by using mitochondria depleted of exchangeable anions. Measurements of ¹⁴C-labelled oxoglutarate in the mitochondrial pellet in the presence or in the absence of (displacing) inhibitor permit the calculation of the bound oxoglutarate.

The binding curve shows cooperative effects similar to but not identical with those reported for the kinetic-saturation curve.

These results have been briefly presented elsewhere [22–24].

MATERIALS AND METHODS

Materials

Special reagents were obtained as follows: 2-oxo[5-¹⁴C]-glutarate, [U-¹⁴C]sucrose and tritiated water (The Radiochemical Center, Amersham, England); rotenone (Sigma Chemical Company, Saint-Louis, MO, U.S.A.); mersalyl, acid form (Mann Research Laboratories, New York, U.S.A.); phenylsuccinate (Aldrich, Milwaukee, WI, U.S.A.). Aqueous solutions of 2-oxo[5-¹⁴C]glutarate are stable for a month if kept, unfrozen, in melting ice.

Preparation and Preloading of the Mitochondria for Kinetic and Binding Experiments

Rats were 200–250-g fed males from inbred strains of Wistar R/A Pfd f. Mitochondria from rat-heart ventricles were prepared according to Tyler and Gonze [25]; the isola-

tion medium contains: 225-mM mannitol, 75-mM sucrose and 0.05-mM EDTA, neutralized with 1-M Tris. Mitochondria were usually loaded with malate (total malate = 2 to 6 μmol/ml of mitochondrial matrix) to eliminate the other exchangeable dicarboxylates. This was achieved by a 30-min incubation at 0 °C in the following medium: 184.5-mM mannitol, 61.5-mM sucrose, 20 mM Tris/Cl buffer pH 7.4, 0.041-mM EDTA and 5-mM malate (first mitochondrial preparation). Higher internal-malate levels (> 6 μmol/ml of mitochondrial matrix) were obtained by a 5-min incubation of the mitochondria at 25 °C in the same medium supplemented with 5-mM or 10-mM malate and 4 μg of rotenone per ml (second mitochondrial preparation). Lower and very low internal-malate levels (from 1 to 0.05 μmol/ml of mitochondrial matrix) were obtained by incubating malate-loaded mitochondria during a 1–10-min period at 25 °C in a malate-free medium containing 8.33-mM KCl, 2.77-mM MgCl₂, 1.11-mM EDTA, 27.7-mM Tris/Cl buffer pH 7.4, 0.55-mM arsenite, 0.11-mM mersalyl, 12.5 μg of rotenone per ml, 112.5-mM mannitol and 37.5-mM sucrose, and cooling them by dilution in a large volume of the ice-cold isolation medium of Tyler and Gonze (third mitochondrial preparation); the three inhibitors (arsenite, mersalyl and rotenone) were proved necessary to obtain very low malate levels.

The three mitochondrial preparations were then centrifuged; the pellets were resuspended in a large volume (100:1) of the ice-cold isolation medium of Tyler and Gonze to eliminate the malate added or released and thus present in the sucrose-accessible space, and recentrifuged. The malate level of the three mitochondrial preparations may be reduced by successive washings in larger volumes (300:1) of the same ice-cold isolation medium and centrifuged. All mitochondrial preparations were finally resuspended in a small volume containing 10 mg of mitochondrial protein/ml (0.5 mg/50-μl aliquot).

Binding experiments were made exclusively with malate-depleted mitochondria (third mitochondrial preparation) washed three times; their internal-malate level was the lowest one measurable (10 nmol/ml of mitochondrial matrix).

The concentrations of the other exchangeable dicarboxylates in these mitochondrial preparations were measured and found to be negligible (less than 3% of the malate in loaded mitochondria and undetectable in unloaded mitochondria). These dicarboxylates were determined enzymatically with a double-beam dual-wavelength Aminco/Chance spectrophotometer at 350–375 nm: oxoglutarate [26], oxaloacetate [27], malate was determined by a modification of Hohorst's procedure [28], as suggested by E. J. Davis (personal communication to Meijer [29]), the displacement being achieved, not by hydrazine, but by coupling with acetyl-CoA in the presence of citrate synthase.

Mitochondrial protein was determined by the biuret method [30] using bovine-serum albumin (fraction V) as a standard. The mitochondrial-matrix volume and the sucrose-accessible space were calculated from the content of mitochondrial pellets in tritiated water and ¹⁴C-labelled sucrose in parallel assays [3].

Incubation Medium

The incubation medium contained 15-mM KCl, 5-mM MgCl₂, 2-mM EDTA, 50-mM Tris/Cl buffer pH 7.4, 22.5-mM mannitol, 7.5-mM sucrose, 4 μg of rotenone per ml, 1-mM arsenite, 0.2-mM mersalyl and 6.67 μCi (247 kBq) of tritiated water per ml. The mitochondrial protein was determined, around 0.5 mg in an incubation assay of 0.5 ml. The final concentration of phenylsuccinate, inhibitor of the translocation, was 22.7 mM and this produced a 98% inhibition. The temperature was 2 °C.

Kinetic Studies

at Very Low External-Substrate Concentrations

Experimental timing, equipment and requirements for kinetic studies have been described in [10]; let us add however that the internal-malate content does not vary during the 1-min preincubation at 2°C (required for 'equilibration') preceding the addition of the labelled substrate.

Kinetic experiments at very low external-substrate concentrations (< 1 μM) require incubations of particularly short duration since the external-substrate concentration would otherwise fall to an extent incompatible with initial-rate determinations. Incubation times should therefore not exceed 1 s and the zero-time value should not be that given by simultaneous injections of substrate and inhibitor since a lag period is observed below 0.2 s. The slope should be calculated from the best-fitting straight line of points corresponding to incubation times between 0.2 and 1 s.

Fig. 1 shows the oxoglutarate in the mitochondrial pellet as a function of the incubation time, i.e. the time between the successive addition of oxoglutarate first, phenylsuccinate second. The circle on the Y axis is obtained by simultaneous addition of substrate and inhibitor. It corresponds to (a) the oxoglutarate in the sucrose-accessible space, (b) the oxoglutarate bound to the membrane in the presence of the inhibitor, and (c) the oxoglutarate having entered the mitochondrial matrix in the presence of the inhibitor, at a rate of 2% of the non-inhibited exchange.

This experimental value is higher than that obtained by linear extrapolation of the other experimental values. This indicates an induction time τ due to a lower rate of exchange during the transient phase than during the subsequent steady state. The value of τ diminishes as the substrate concentration increases from 0.2 to 3.3 μM (not shown); at higher concentrations, τ is too small to be determined accurately with our present technique.

Smoothing the Experimental Curves

The best-fitting straight line is calculated from the coordinates of each set of three consecutive experimental points. The adjusted ordinate of the middle points is obtained by introducing its abscissa in the corresponding equation; the same procedure is also used for the first and last points of the series. This process may be repeated several times if needed. The smoothed curve is that passing through the thus adjusted values.

BINDING EXPERIMENTS

Principles

From the previous studies [3,4,10] confirmed in this article (see below) we know that the substrates bound to the translocator are in equilibrium with their soluble forms on both sides of the membrane and that the binding to the outer face of the membrane is independent of the concentration of internal substrates.

When mitochondria are incubated in the presence of ¹⁴C-labelled oxoglutarate, the total radioactivity found in the pellet after centrifugation is the sum of (a) OG^s : the oxoglutarate having diffused into the sucrose-accessible space of which the external membrane is part, (b) OG^b : the oxoglutarate bound to the outer face of the internal membrane, and (c) OG^m : the oxoglutarate having penetrated the internal membrane and bound to the inner face of that membrane, and that having penetrated into the matrix space.

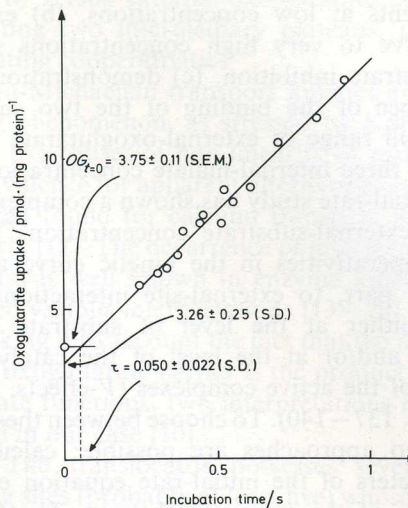


Fig. 1. Initial rate of oxoglutarate uptake by malate-loaded mitochondria. Mitochondria: 0.56 mg of protein. Exchange reaction initiated by addition of 0.31-μM oxoglutarate and stopped by addition of 22.7-mM phenylsuccinate. The internal-malate concentration is 4 mM. The experimental point (circle) on the Y axis is the mean (\pm S.E.M.) of 16 determinations (substrate and inhibitor added simultaneously); τ is the abscissa of the intersection between the least-square straight line obtained for the other oxoglutarate uptakes as a function of time and the horizontal line passing through the $OG_{t=0}$ circle; the standard deviation of the τ -value is calculated as:

$$s^2(\tau) = \frac{1-r^2}{n-2} \left[\frac{n-1}{n-2} + \frac{(y^* - \bar{y})^2}{s^2(y)} \right] s^2(x)$$

where r is the correlation coefficient, x the incubation time, y the oxoglutarate uptake, y^* the ordinate for $x = 0$ and n the number of experimental points

If a competitive but non-penetrating inhibitor of the transport is added afterwards it displaces the oxoglutarate bound to the sites accessible to the inhibitor, i.e. that which is bound to the outer face of the membrane; the displaced oxoglutarate is released. The oxoglutarate bound to the outer face of the membrane may thus be determined by difference.

Phenylsuccinate is such a competitive and non-penetrating inhibitor (verified in our laboratory). Even at the high concentration used the transport continues at about 2% of the original non-inhibited rate, implying that about 2% of the oxoglutarate remains bound to the outer face of the membrane, accessible to the inhibitor. This residual uptake and binding must be accounted for.

Experimental Procedure

It is essential to determine the oxoglutarate present in the sucrose-accessible space (OG^s) with the highest possible accuracy because of the size of its contribution to the total radioactivity of the pellet (OG^t) as shown in Table 1. The sucrose-accessible space (V^s) must be determined in parallel with all incubation assays using ¹⁴C-labelled sucrose and unlabelled oxoglutarate. OG^s is equal to $V^s \cdot [OG]_0$ where $[OG]_0$ is the initial external-oxoglutarate concentration.

Strictly speaking the final external-oxoglutarate concentration should be used instead of $[OG]_0$ since a small fraction of the initial external oxoglutarate is taken up from the suspension medium during the incubation. Thus V^s should be

multiplied by $\{[OG]_0 - (OG^b + OG^m)/V^e\}$ where V^e is the non-matrix volume of the total incubation assay. Thus,

$$OG^t = V^s \{[OG]_0 - (OG^b + OG^m)/V^e\} + OG^b + OG^m \\ = V^s [OG]_0 + (OG^b + OG^m) \left(1 - \frac{V^s}{V^e}\right).$$

Since V^s/V^e is in practice less than 0.003, it may be neglected.

All subsequent calculations are made on the total oxoglutarate of the pellet from which the oxoglutarate in the sucrose-accessible space has been subtracted, thus on $OG^t - OG^s$.

The necessary experiments are described below and their timing is illustrated in Fig. 2.

Experiment A. After 1-min preincubation, 0.15 ml of oxoglutarate, dissolved in the incubation medium, is vigorously added to 0.35 ml of a suspension containing 0.3 ml of incubation medium and 0.05 ml of the final mitochondrial preparation; this ensures immediate homogenisation (see [10]). Centrifugation starts exactly 60 s later, in an Eppendorf microcentrifuge (model 3200, 16000 rev./min). The mean sedimentation time of 26 s (see below) added to the 60-s pre-centrifugation time gives the actual incubation time: 86 s. The difference ($OG^t - OG^s$) in experiment A (OG_A) may be written:

$$OG_A = OG_{86}^b + OG_{86}^m. \quad (1)$$

In this and subsequent equations the numerical subscript indicates the duration of the incubation in seconds (here 86); the capital-letter subscript refers to the experiment type (here A).

Experiment B. After 1-min preincubation, the oxoglutarate is added vigorously as described in experiment A. This is followed, 86 s later, by vigorous injection of 0.2 ml of 80-mM phenylsuccinate dissolved in water and by centrifugation 7 s later (this is arbitrary but convenient for experimental purposes). Thus,

$$OG_B = OG_{119}^{b'} + OG_{86}^m + OG_{33}^{m'}. \quad (2)$$

In this and subsequent equations, the prime sign (') is used to indicate the presence of the competitive inhibitor phenylsuccinate which reduces both the binding to the outer face of the membrane and the rate of the catalysed exchange. The addition of the inhibitor also reduces the external-substrate concentration by 28.4%; this is taken into account for the calculation of OG^s : $[OG]_0$ is replaced by $0.716 \times [OG]_0$. The osmolarity of the solution of phenylsuccinate is somewhat higher than the osmolarity of the incubation medium and modifies the size of the sucrose-accessible space but, as indicated before, the latter is determined in parallel with all incubation assays.

Experiment C. This is made to take into account the residual binding and exchange in the presence of the inhibitor. After 1-min preincubation, oxoglutarate and phenylsuccinate are added simultaneously, followed by centrifugation 7 s later. Thus,

$$OG_C = OG_{33}^{b'} + OG_{33}^{m'}. \quad (3)$$

Calculations

Eqn (4) = (1) + (3) - (2) gives:

$$OG_A + OG_C - OG_B \\ = OG_{86}^b + OG_{33}^{b'} + OG_{86}^m + OG_{33}^{m'} \\ - OG_{119}^{b'} - OG_{86}^m - OG_{33}^{m'} \\ = OG_{86}^b + (OG_{33}^{b'} - OG_{119}^{b'}) + (OG_{33}^{m'} - OG_{33}^{m'}). \quad (4)$$

As indicated now, $(OG_A + OG_C - OG_B)$ gives a reasonable estimation of OG_{86}^b because the additional terms in Eqn (4) are negligible.

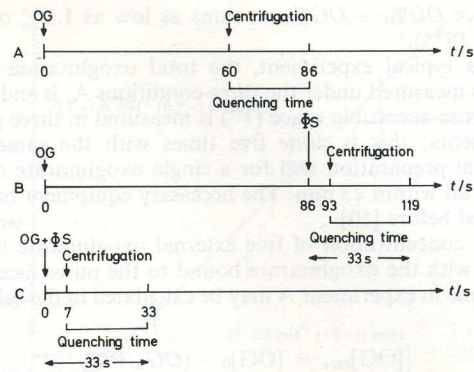


Fig. 2. Experimental scheme. OG, oxoglutarate; ϕS , phenylsuccinate

$OG_{33}^{b'}$ and $OG_{119}^{b'}$ may differ because the external oxoglutarate concentration with which they are in equilibrium are not exactly the same after 33-s incubation in the presence of inhibitor, or after 86-s incubation without inhibitor followed by 33-s incubation in the presence of inhibitor. The difference between these concentrations was found not to exceed 6% in the most unfavourable conditions (lowest external-oxoglutarate concentrations). The oxoglutarate taken up during the incubation is of course replaced by equal amounts of malate, the presence of which will affect the binding of oxoglutarate. Even if we assume that malate binds to the translocator with the same affinity as oxoglutarate (previous experiments [4] have shown that its apparent affinity is in fact one-fifth of that of oxoglutarate in that range of concentrations) $OG_{119}^{b'}$ will be 12% less than $OG_{33}^{b'}$; however $OG_{119}^{b'}$, be it after 33 or 119 s, represents only 2% of OG^b . The term ($OG_{33}^{b'} - OG_{119}^{b'}$) is therefore not larger than 0.24% of OG^b .

$OG_{33}^{m'}$ and OG_{33}^{m} may differ because the oxoglutarate transported in the presence of the inhibitor is not the same when this is added at t_0 (experiment C) or at t_{86} (experiment B) since the external and internal concentrations of the substrates regulating the exchange become lower in experiment B than in experiment C when the concentrations of the products of the exchange become higher. The external-oxoglutarate concentration in experiment B was found not to be less than 94% of that in experiment C under the most unfavourable conditions (lowest external-oxoglutarate concentrations). One would expect the internal-malate concentration to be reduced as much as 60% in the most unfavourable conditions (high external-oxoglutarate concentrations) but this is not the case since the presence of endogenous aspartate in the mitochondrial matrix continuously regenerates the extruded malate; the oxoglutarate taken up transaminates with aspartate to produce oxaloacetate which is further reduced to malate; the disappearance of aspartate is equal to the entry of oxoglutarate and the malate concentration does not change (unpublished results). For the same reasons the oxoglutarate taken up (internal product of the reaction) does not appear in the matrix space from where it could inhibit the transport. The concentration of external malate (external product of the reaction) is less than 0.1% of the highest external-oxoglutarate concentration and does not exceed 6% of the lowest external-oxoglutarate concentration; in any case the external-malate concentration never reaches more than 0.06 μM which is small compared with its dissociation constant, 11.6 μM [4] and has no significant effect on the uptake of oxoglutarate. The decrease of external-oxoglutarate concentration alone (6%) can affect, by 6% (very roughly) its uptake in $OG_{33}^{m'}$ compared to OG_{33}^m and only at the lowest external-oxoglutarate concentrations. $OG_{33}^{m'}$ may be as high as 18% of OG_{86}^b but the

difference $OG_{33C}^m - OG_{33B}^m$ remains as low as 1.1% of OG_{86}^b (6% of 18%).

In a typical experiment, the total oxoglutarate uptake (OG^t) is measured under the three conditions A, B and C, and the sucrose-accessible space (V^s) is measured in three parallel experiments: this is done five times with the same mitochondrial preparation and for a single oxoglutarate concentration, all within 23 min. The necessary equipment has been described before [10].

The concentration of free external oxoglutarate in equilibrium with the oxoglutarate bound to the outer face of the membrane in experiment A may be calculated in the following way:

$$[OG]_{free} = [OG]_0 - (OG_A/V^s).$$

Table 1 illustrates experiments made at four different concentrations of external oxoglutarate.

Requirements

The elaboration of the experimental procedure described required preliminary controls.

Incubation Time. The incubation time of 86 s in experiments A and B was selected to reduce errors of timing. Fig. 3 shows a rapid uptake of oxoglutarate lasting about 1 s, at a rate of $3.9 \text{ pmol} \times \text{s}^{-1} \times (\text{mg protein})^{-1}$ followed by a slower accumulation at a rate of $0.16 \text{ pmol} \times \text{s}^{-1} \times (\text{mg protein})^{-1}$. The incubation time was interrupted during the slow accumulation.

Centrifugation Quenching Time. The centrifugation quenching time must be determined accurately. It is part of the total incubation time in experiment A (60 s + quenching time) which must be equal to the time preceding the addition of phenylsuccinate in experiment B. The quenching time may be obtained by plotting $OG^t - OG^s$ as a function of the time interval between addition of oxoglutarate and onset of the centrifugation. The rate of uptake must be lowered to be linear for about 1 min and thus permit linear extrapolation back to the axis of the abscissae. This had been achieved previously by incubating mitochondria in the presence of phenylsuccinate; a quenching time of 25.7 ± 0.9 s was ob-

tained [10]. Since phenylsuccinate had been used at high concentration, the mitochondrial pellet had somewhat shrunk, possibly as a result of the slight increase in osmolarity. Experiments made in the presence of malate, a more efficient competitor of the exchange (and thus effective at 1-mM concentration), have led to a new figure of 25.0 ± 2.5 s. We have assumed the centrifugation quenching time to be 26 s. In the presence of malate or phenylsuccinate OG^b is a negligible part of $OG^t - OG^s$.

External-Product Inhibition. External oxoglutarate enters the matrix space in exchange for internal malate, so that the external solution contains more and more malate competing with the oxoglutarate for the external binding sites. The final $[\text{malate}]_{out}/[\text{oxoglutarate}]_{out}$ ratio is high only when the initial external-oxoglutarate concentration is low: calculation shows that, in experiments A and B, the ratio is about 0.05, 0.02 or

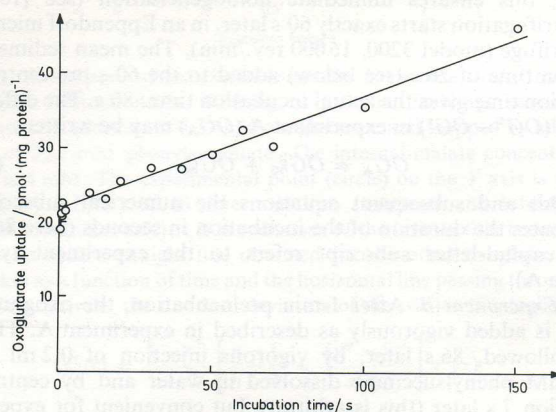


Fig. 3. Oxoglutarate uptake by malate-depleted mitochondria. Malate-depleted mitochondria (0.51 mg of protein) contained 30- μM malate. The incubation time represents the interval between the injections of ^{14}C -labelled oxoglutarate (4.83- μM) and phenylsuccinate. The oxoglutarate uptake is not corrected for the sucrose-space contamination nor for the residual uptake after addition of the inhibitor

Table 1. Bound and free oxoglutarate as a function of initial external oxoglutarate concentration, $[OG]_0$

Malate-depleted mitochondria (0.52 to 0.58 mg of protein) are incubated with labelled oxoglutarate in three different experiments (A, B, and C) described in Fig. 2 and the oxoglutarate found in the mitochondrial pellet (OG^t) is measured; under condition C, the initial-oxoglutarate concentration is 0.716-times that prevailing under conditions A and B. In parallel assays, the sucrose space (V^s) is determined in order to calculate the oxoglutarate in this space (OG^s). Calculated from these values: OG^m , translocated oxoglutarate; OG^b , bound oxoglutarate; $[OG]_{free}$, free external-oxoglutarate concentration. Means \pm S.E.M. ($n = 5$)

$[OG]_0$	Expt	$[OG]_{free}$	V^s	OG^t	OG^s	OG_{86}^m	OG^b
μM		μM	μl	$\text{pmol} \times (\text{mg protein})^{-1}$			
0.69	A	0.67	1.67	20.80 ± 1.02	2.16 ± 0.02	15.78 ± 0.75	2.86 ± 0.8
	B		1.49	17.95 ± 0.74	1.38 ± 0.01		
	C		1.43	2.11 ± 0.11	1.32 ± 0.01		
4.68	A	4.63	1.81	67.21 ± 0.65	15.95 ± 0.12	39.10 ± 0.82	12.2 ± 0.9
	B		1.64	54.64 ± 0.35	10.33 ± 0.03		
	C		1.53	14.89 ± 0.73	9.67 ± 0.01		
20.95	A	20.9	1.88	142.30 ± 1.27	68.40 ± 0.76	48.90 ± 2.48	25.0 ± 2.9
	B		1.83	99.58 ± 1.00	47.69 ± 0.81		
	C		1.71	47.66 ± 1.90	44.67 ± 0.96		
85.9	A	85.7	1.44	359.12 ± 4.72	237.92 ± 5.19	56.44 ± 4.00	64.8 ± 3.5
	B		1.34	223.78 ± 2.96	158.15 ± 1.33		
	C		1.32	165.57 ± 1.60	156.38 ± 1.70		

0.005 when the initial external-oxoglutarate concentration is 0.1, 1 or 10 μM respectively (lower concentrations were not used). Since the affinity of the translocator for malate is one order of magnitude less than for oxoglutarate (see respective K_m -values in [4]), the displacement of oxoglutarate by malate will never be more than a fraction of 5% under the most unfavourable conditions, i.e. much less than the 5–10% relative standard error of the bound oxoglutarate under similar conditions.

Substrate Concentrations. The upper limit of the external-oxoglutarate concentration is approximately 200 μM since the oxoglutarate in the sucrose-accessible space (OG^s) becomes a too large fraction of the total oxoglutarate of the pellet (OG^p) otherwise. The internal-malate concentration must be as low as possible to reduce the size of the exchanged oxoglutarate (OG^m) but need not be the same for different external-oxoglutarate concentrations: it was kept below 50 μM .

The high degree of reproducibility of the results has permitted us to construct kinetic (82 points) and binding (57 points) curves from a large number of mitochondrial preparations over a long period of time. This is probably because:

- the animals are a pure strain coming from the same breeder and always weigh between 200 and 250 g;
- each mitochondrial preparation is made of at least eight rat hearts; individual variations are already averaged;
- mitochondria are prepared in exactly the same way using the same equipment by the same manipulator;
- the preloading to known internal-malate concentration makes the preparations more homogenous; the internal exchangeable anions have all disappeared except for malate; other non-exchangeable dicarboxylates such as aspartate and glutamate are not eliminated but their concentration is essentially constant in our preparations;
- the sucrose-accessible space is normally $56.2\% \pm 0.4$ (S.D.) for malate-loaded mitochondria (kinetics) and $65.1\% \pm 0.5$ (S.D.) for unloaded mitochondria (binding); the results obtained with mitochondria having a sucrose-accessible space higher than 63% for kinetics and 72% for binding are not used for the drawing of the curves because underestimated values are obtained as discussed in [31].

RESULTS AND DISCUSSION

Initial Rate versus Internal-Malate Concentration

The dependence of the rate of the oxoglutarate_{out}/malate_{in} exchange on the internal-malate concentration has now been investigated between 0.1 and 11-mM concentration for a single external concentration of oxoglutarate (4.84 μM) convenient for radioactivity measurements. A hyperbola-like saturation curve is observed for initial rate versus internal-malate concentration (not shown).

However the double-reciprocal plot is made of two straight-line segments (Fig. 4). Segment I corresponds to concentrations ranging from 1 to 11 mM, i.e. to those concentrations that had been used in previous experiments [10]. Segment II corresponds to concentrations lower than 1 mM, down to 0.1 mM. The saturation curve for internal malate thus deviates from a pure Michaelian law and indicates an apparent positive cooperativity (Lineweaver-Burk plot curved upwards, see p. 137 in [21]).

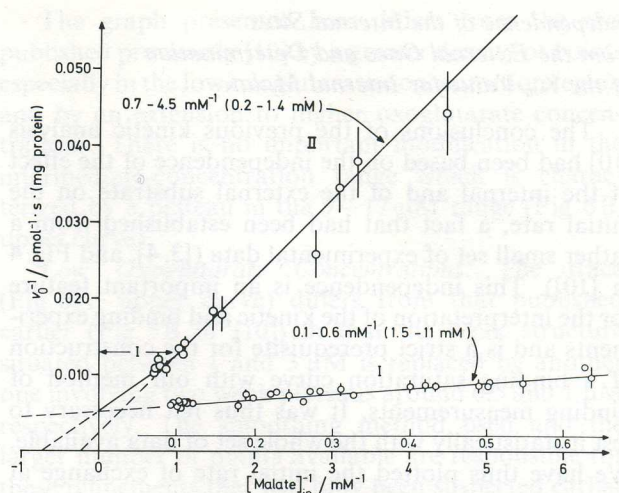


Fig. 4. Reciprocal of the initial rate of exchange as a function of the reciprocal of the internal-malate concentration at 4.84- μM external-oxoglutarate concentration. Malate-loaded mitochondria (0.42 to 0.57 mg of protein) are prepared to obtain an extended range of malate concentrations, as described in Materials and Methods. Each point is obtained by measuring the rate (slopes calculated from five incubation times) at 4.84- μM external oxoglutarate; vertical bars represent the standard deviations. The trace passes through the adjusted points (not shown) obtained by the smoothing method described

The existence of a positive cooperativity cannot be explained by the existence of independent internal sites of different affinities for malate [31a] since the high-affinity sites would be saturated first, thus leading to negative cooperativity (Lineweaver-Burk plot curved downwards). Interacting internal sites could explain the positive cooperativity.

The deviation from Michaelian behaviour could however be artefactual and due to one of the two following explanations that cannot be ruled out.

a) The internal free malate is only part of the $[\text{malate}]_{\text{in}}$ on the abscissae of Fig. 4; the malate bound to the translocator and to those enzymes that can combine with malate would no longer be negligible, compared to the free malate, at low internal-malate concentrations.

b) The treatment suffered by the mitochondria to obtain very low internal-malate concentrations modifies the internal concentration of a substance that is an effector of the translocation.

If the deviation from Michaelian behaviour is due to interaction between internal sites or to the existence of still unknown effectors, than K_m -values calculated from either segment I or segment II would be apparent only. If the deviation is due to having neglected the bound malate (the most likely explanation indeed), and thus if kinetics is Michaelian, then K_m can only be calculated from segment I and gives the true dissociation constant of the translocator-malate_{in} complex since the kinetics is of the rapid-equilibrium type [3, 4] (this paper).

*Independence of the Internal Sites
from the External Ones and Determination
of the K_m -Value for Internal Malate*

The conclusions of the previous kinetic analysis [10] had been based on the independence of the effect of the internal and of the external substrate on the initial rate, a fact that had been established from a rather small set of experimental data ([3, 4], and Fig. 4 in [10]). This independence is an important feature for the interpretation of the kinetic and binding experiments and is a strict prerequisite for the construction of a binding saturation curve with our method of binding measurements. It was thus felt necessary to test it statistically with the whole set of data available. We have thus plotted the initial rate of exchange at 2-mM internal malate as a function of the rate at 6-mM internal malate for 75 different external-oxoglutarate concentrations ranging from 0.08 to 248 μM . This is shown in Fig. 5 where low rates correspond to low external-oxoglutarate concentrations.

The expected relation to be tested is a straight line passing through the origin. The independence of the effects of the two substrates means that the initial rate is the product of two functions, f and g , each depending on one substrate only so that for one given external-oxoglutarate concentration:

$$v_0(2) = f([\text{OG}]) \cdot g([\text{Mal}]_2)$$

and

$$v_0(6) = f([\text{OG}]) \cdot g([\text{Mal}]_6)$$

where $v_0(2)$ and $v_0(6)$ represent the initial rates of exchange at 2 and 6-mM internal malate respectively.

The ratio $v_0(2)/v_0(6)$ does not depend on the external-oxoglutarate concentration chosen and

$$v_0(2) = \frac{g([\text{Mal}]_2)}{g([\text{Mal}]_6)} \times v_0(6)$$

which, in the case of a g function being Michaelian becomes

$$v_0(2) = \frac{[\text{Mal}]_2}{[\text{Mal}]_6} \times \frac{[\text{Mal}]_6 + K_m}{[\text{Mal}]_2 + K_m} \times v_0 \quad (6).$$

The Michaelis constant for the internal malate may thus be calculated from the slope (a) of the straight line:

$$K_m = \frac{[\text{Mal}]_2 [\text{Mal}]_6 (a - 1)}{[\text{Mal}]_2 - a[\text{Mal}]_6}$$

The data in Fig. 5 cover a rather narrow sector of the graph, with the exception of seven of them (filled circles) obtained above 60- μM external oxoglutarate. If these unexplained figures are excluded (see legend of Fig. 5) a regression line may be calculated; its equation is $y = (0.74 \pm 0.02)x + (2.92 \pm 3.01)$. The variable of Student is equal to 43; the correlation coefficient is equal to 0.983. The linear regression is therefore highly satisfactory, demonstrating the independence of the internal sites from the external ones.

The K_m (\pm S.D.) for internal malate may be calculated from this plot and this gives 1.30 ± 0.14 mM.

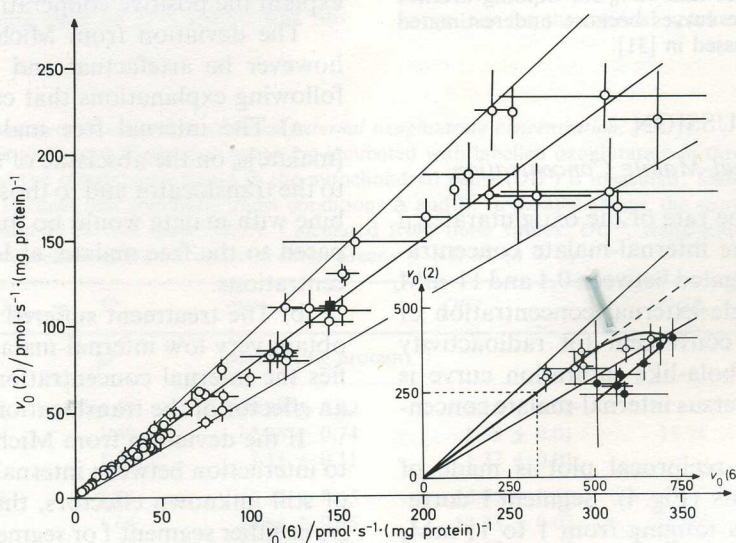


Fig. 5. Initial rate of exchange, at 2-mM internal malate or $v_0(2)$, as a function of the rate at 6-mM internal malate, or $v_0(6)$. The external-oxoglutarate concentration extends from 0.08 μM to about 50 μM (highest rate) and 250 μM (inhibited rates). The open circles and perpendicular bars represent the means (\pm S.D.) of figures obtained by linear interpolation or slight extrapolation of the double-reciprocal plots of the rates (\pm S.D.) obtained with three or more internal-malate concentrations, of which one was close to 2 mM, another one close to 6. The figure illustrated by a filled square is the one obtained by the experiments of Fig. 4. The filled circles correspond to experiments made at concentrations higher than 60- μM external-oxoglutarate concentration at which excess-substrate inhibition starts; the measurements are less accurate under such conditions (high OG^s); their being all deviated-downwards suggests an additional but unknown cause of systematic error

K_m^{-1} for internal malate has also been calculated by extrapolation, in Fig. 4, of segment I to the axis of abscissae, and a mean (\pm S.D.) value of $0.75 \pm 0.04 \text{ mM}^{-1}$ has been obtained; this corresponds to a K_m -value of $1.33 \pm 0.08 \text{ mM}$. The standard deviation is particularly low because segment I comprises 39 experimental points.

The two K_m -values obtained independently (1.30 ± 0.14 and 1.33 ± 0.08) are in very close agreement but differ from those obtained previously on smaller populations of data, using different mathematical treatment.

a) $2.94 \pm 0.73 \text{ mM}$ [3] was obtained by extrapolation of nine converging straight lines (reciprocal plots) defined by three points each (thus 27 points) imposing a common but unknown point of intersection on the axis of abscissae. The calculation (see appendix to [4]) had involved an inversion of the coordinates X and Y . In such a calculation involving the regression of X over Y , the mean value is higher than that obtained in the regression of Y over X ; indeed, if the K_m is recalculated from those data by averaging the points of intersection of the nine best-fitting straight lines directly with the axis of abscissae (without inversion of the coordinates), a figure of $2.30 \pm 0.94 \text{ mM}$ is obtained, not statistically different from those given above (1.30 ± 0.14 and $1.33 \pm 0.08 \text{ mM}$ respectively).

b) $2.43 \pm 0.32 \text{ mM}$ [10] was obtained by extrapolation of seven converging lines (reciprocal plots) defined by 10 points each (thus 70 points) by the same type of calculation. Direct calculation of the mean of the points of intersection of the seven regression lines with the axis of abscissae gives $1.61 \pm 0.51 \text{ mM}$, again not statistically different from those given above.

The latest figure, with the smallest standard deviation given in this paper and obtained from two entirely independent sets of data is presumably the most reliable one.

Influence of the External-Oxoglutarate Concentration on the Initial Rate

The experimental scheme described in [10] permits, with a single mitochondrial preparation, measurement of the initial rate of exchange for three chosen external-oxoglutarate concentrations and three internal-malate concentrations, usually between 1.5 and 8 mM. For one oxoglutarate concentration we can calculate the least-square straight line of the double reciprocal plots (v_0^{-1} versus $[\text{malate}]^{-1}$) from which one obtains rates for three chosen internal-malate concentrations: 2, 4 and 6 mM.

The initial rates of the exchange $\text{oxoglutarate}_{\text{out}}/\text{malate}_{\text{in}}$ at a fixed internal-malate concentration of 4 mM for different oxoglutarate concentrations between 0.08 and 293 μM are presented in Fig. 6A—C (upper curve).

The graph presented here differs from the one published previously [10] by a greater density of points especially in the low oxoglutarate-concentration region and by an extension to higher oxoglutarate concentrations. There is no important modification in the intermediate-concentration range which is characterized by a plateau in the 9–17- μM range (Fig. 6B, upper curve).

Low Oxoglutarate Concentrations. The trace (Fig. 6A, upper curve) differs from that published earlier (Fig. 5B of [10]) in that the weak structure situated between 1 and 3 μM is replaced by another one involving two weak plateaus around 0.5 and 1 μM respectively. The smoothing method used and the larger number of points available are responsible for these refinements that had only been suspected earlier and had in fact been incorrectly interpreted [10]: the deviation at low external-oxoglutarate concentration had been used to estimate the translocator concentration but this is no longer tenable for the bound oxoglutarate is a very small fraction of the added oxoglutarate, even at those low concentrations (see below).

High Oxoglutarate Concentrations. At high external-oxoglutarate concentrations, a significant decrease of the exchange rate is observed (Fig. 6C, upper curve), beyond a rather wide plateau. This inhibition may be due to the binding of another oxoglutarate molecule to each catalytic site or to the binding of oxoglutarate on inhibitory sites, constraining or preventing the conformational changes implied in the exchange function of the translocator-substrates complexes.

Influence of Internal Malate on the Kinetic-Saturation Curve by External Oxoglutarate

The initial rates, for each external-oxoglutarate concentration, calculated for 2, 4 and 6-mM internal malate are not independent from each other since they are obtained from the best-fitting straight line linking three experimental rate determinations. Each triplet of calculated rates is however independent of the other triplets obtained at other oxoglutarate concentrations because a common point of intersection on the axis of abscissae is not imposed for the calculation of the straight lines (v_0^{-1} versus $[\text{malate}]^{-1}$).

Fig. 7 shows the three rate curves (v_0^{-1} versus $[\text{oxoglutarate}]^{-1}$) for the three chosen concentrations of internal malate and illustrates the convergence on the axis of abscissae of several pseudolinear parts of the complex curves, as expected if the external and the internal substrate have independent effects on the initial rate. It is to be noticed that a number of apparent K_m and V values could be determined, depending on the substrate-concentration range examined; they would be meaningless.

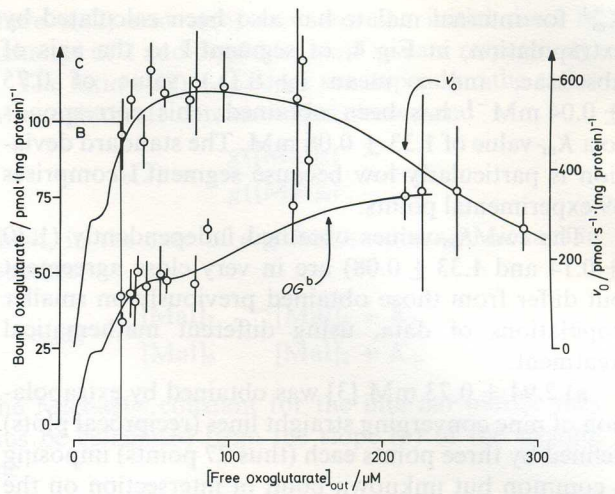
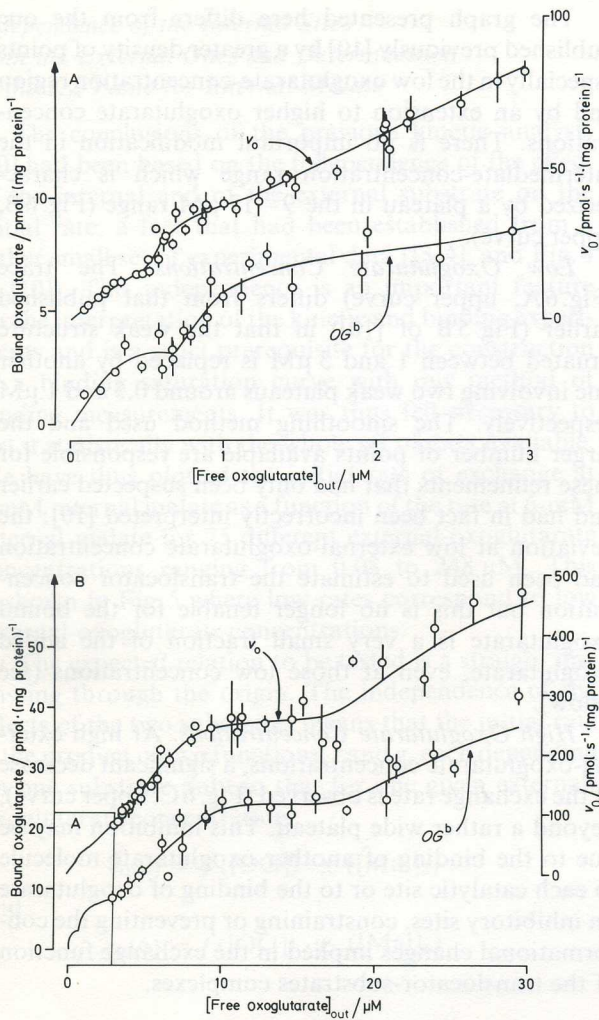


Fig. 6. Bound oxoglutarate (lower curve) and rate of oxoglutarate uptake (upper curve) as a function of free external-oxoglutarate concentration. (Lower curve) malate-depleted mitochondria (0.48 to 0.61 mg of protein); each point is the mean \pm S.E.M. (vertical bar) of five measurements made with the same mitochondrial preparation. (Upper curve) malate-loaded mitochondria (0.41 to 0.57 mg of protein); each point is obtained by linear interpolation of the double-reciprocal plots of the rates obtained with three internal-malate concentrations around 4 mM. Vertical bars represent the standard deviations. Both traces pass through the adjusted points (not shown) calculated by the smoothing method

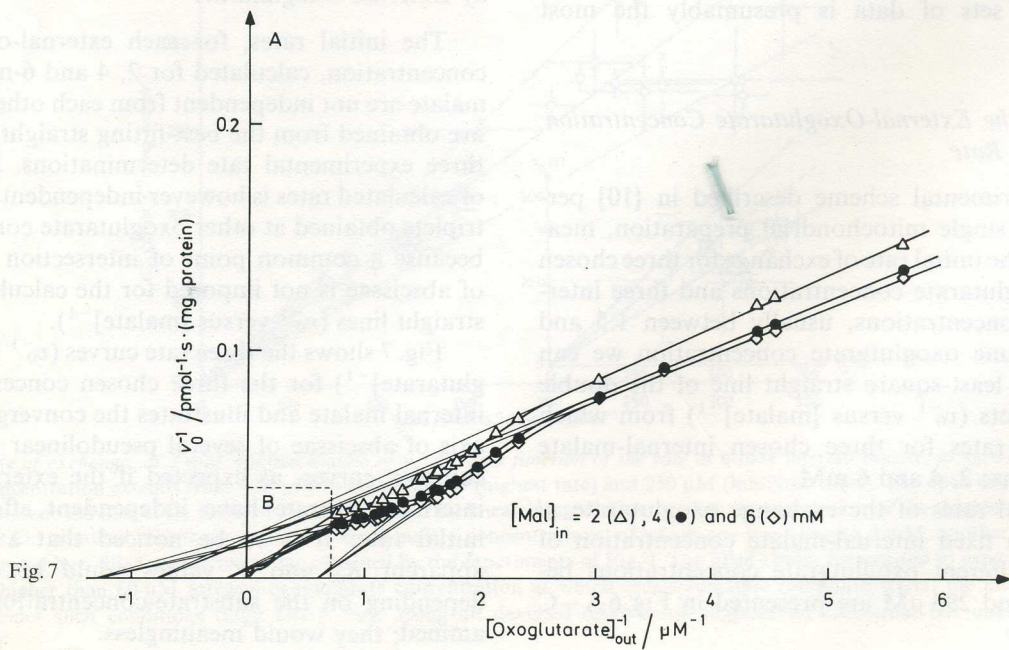


Fig. 7

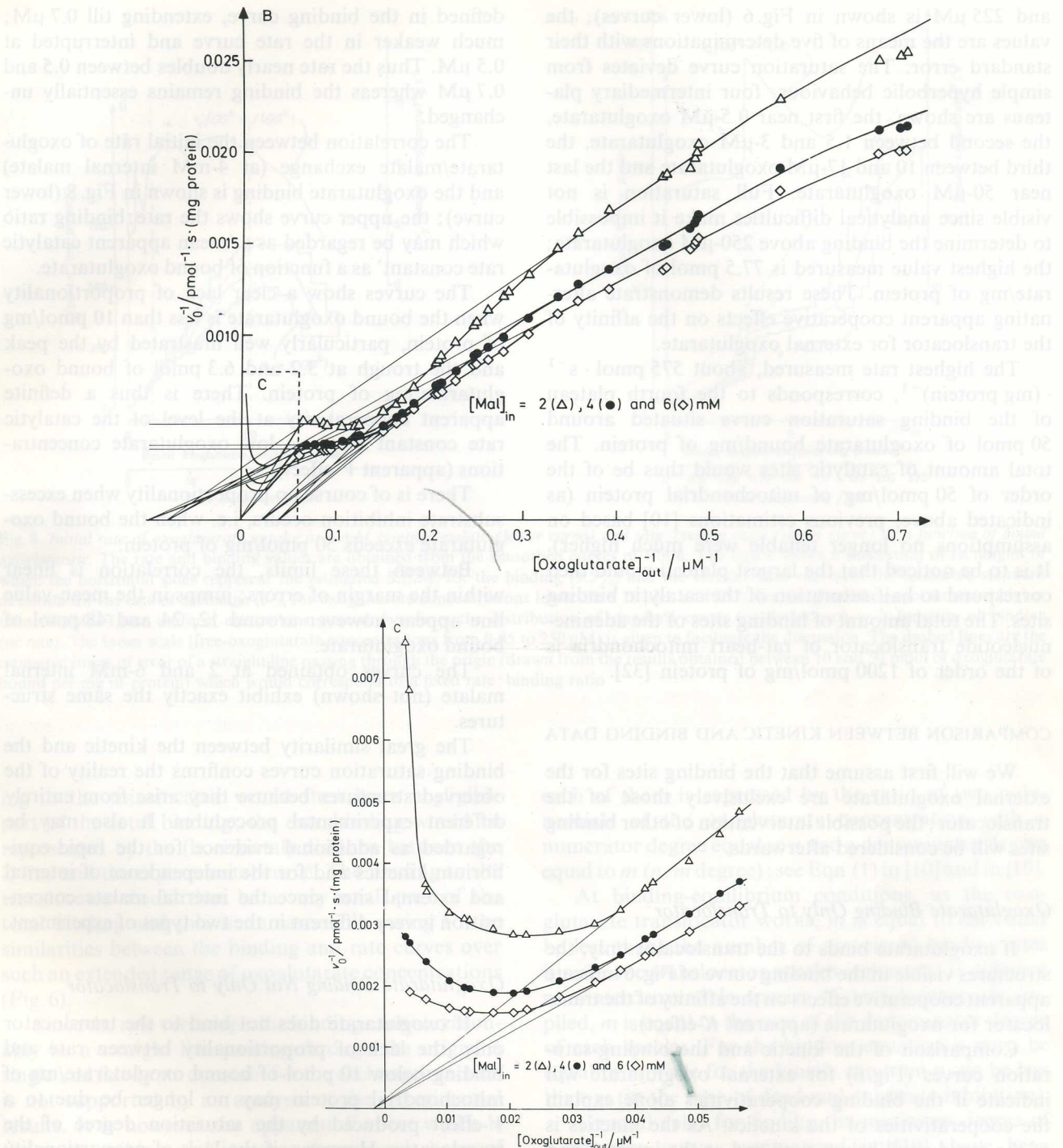


Fig. 7. Reciprocal of the initial rate of exchange as a function of the reciprocal of external-oxoglutarate concentration at 2 (\square), 4 (\bullet), and 6-mM (\diamond) internal malate. The three traces pass through the adjusted points shown calculated by the smoothing method. The middle curve is the reciprocal of the upper curve of Fig. 6

Binding of Oxoglutarate to the Outer Face of the Internal Membrane

It would have been nice to verify directly that the binding of external oxoglutarate is not affected by the concentration of the internal malate but this is impos-

sible since technical reasons require that the OG^m component of the total radioactivity in the pellet be kept as low as possible, as explained in Materials and Methods.

The dependence of the bound oxoglutarate on the free external-oxoglutarate concentration between 0.09

and 225 μM is shown in Fig. 6 (lower curves); the values are the means of five determinations with their standard error. The saturation curve deviates from simple hyperbolic behaviour: four intermediary plateaus are shown, the first near 0.5- μM oxoglutarate, the second between 1.5 and 3- μM oxoglutarate, the third between 10 and 17- μM oxoglutarate and the last near 50- μM oxoglutarate. Full saturation is not visible since analytical difficulties make it impossible to determine the binding above 250- μM oxoglutarate; the highest value measured is 77.5 pmol of oxoglutarate/mg of protein. These results demonstrate alternating apparent cooperative effects on the affinity of the translocator for external oxoglutarate.

The highest rate measured, about $575 \text{ pmol} \cdot \text{s}^{-1} \cdot (\text{mg protein})^{-1}$, corresponds to the fourth plateau of the binding saturation curve situated around 50 pmol of oxoglutarate bound/mg of protein. The total amount of catalytic sites would thus be of the order of 50 pmol/mg of mitochondrial protein (as indicated above, previous estimations [10] based on assumptions no longer tenable were much higher). It is to be noticed that the largest plateau would then correspond to half saturation of the catalytic binding sites. The total amount of binding sites of the adenine-nucleotide translocator of rat-heart mitochondria is of the order of 1200 pmol/mg of protein [32].

COMPARISON BETWEEN KINETIC AND BINDING DATA

We will first assume that the binding sites for the external oxoglutarate are exclusively those of the translocator; the possible intervention of other binding sites will be considered afterwards.

Oxoglutarate Binding Only to Translocator

If oxoglutarate binds to the translocator only, the structures visible in the binding curve of Fig. 6 indicate apparent cooperative effects on the affinity of the translocator for oxoglutarate (apparent *K*-effect).

Comparison of the kinetic and the binding-saturation curves (Fig. 6) for external oxoglutarate will indicate if the binding cooperativities alone explain the cooperativities of the kinetics. As the kinetics is of the rapid-equilibrium type and as the internal and external moieties of the translocator are not interacting, a strict proportionality between the two saturation curves is expected if all the loaded external sites have the same catalytic rate constant whatever the degree of saturation by oxoglutarate may be (identical external sites and no *V*-effect).

Between 1.5 and 75- μM external oxoglutarate, the binding curve resembles the kinetic-saturation curve: three plateaus at the same concentrations of free oxoglutarate. At low oxoglutarate concentrations, a first plateau starts at 0.3- μM oxoglutarate; it is well

defined in the binding curve, extending till 0.7 μM ; much weaker in the rate curve and interrupted at 0.5 μM . Thus the rate nearly doubles between 0.5 and 0.7 μM whereas the binding remains essentially unchanged.

The correlation between the initial rate of oxoglutarate/malate exchange (at 4-mM internal malate) and the oxoglutarate binding is shown in Fig. 8 (lower curve); the upper curve shows the rate:binding ratio which may be regarded as a 'mean apparent catalytic rate constant' as a function of bound oxoglutarate.

The curves show a clear lack of proportionality when the bound oxoglutarate is less than 10 pmol/mg of protein, particularly well illustrated by the peak and the trough at 3.2 and 6.3 pmol of bound oxoglutarate/mg of protein. There is thus a definite apparent cooperativity at the level of the catalytic rate constant at those low oxoglutarate concentrations (apparent *V*-effect).

There is of course no proportionality when excess-substrate inhibition occurs, i.e. when the bound oxoglutarate exceeds 50 pmol/mg of protein.

Between these limits, the correlation is linear within the margin of errors; jumps in the mean-value line appear however around 12, 24 and 48 pmol of bound oxoglutarate.

The curves obtained at 2 and 6-mM internal malate (not shown) exhibit exactly the same structures.

The great similarity between the kinetic and the binding saturation curves confirms the reality of the observed structures because they arise from entirely different experimental procedures. It also may be regarded as additional evidence for the rapid-equilibrium kinetics and for the independence of internal and external sites since the internal malate concentration is very different in the two types of experiment.

Oxoglutarate Binding Not Only to Translocator

If oxoglutarate does not bind to the translocator only, the lack of proportionality between rate and binding below 10 pmol of bound oxoglutarate/mg of mitochondrial protein may no longer be due to a *V*-effect produced by the saturation degree of the translocator. However, if the lack of proportionality is the result of extra binding only, the latter can be subtracted from the total binding and this will shift all the values reported in Fig. 8 and place them on a straight-line passing through the origin (v_0 proportional to the oxoglutarate bound to the translocator). The slope of this line must be at least equal to that of the steepest one in the experimental curve (extra binding cannot diminish when the oxoglutarate concentration increases); the line will thus run parallel to the jump observed at 3.2 pmol of bound oxoglutarate/mg of protein, hence nearly vertical (*Z* line). The bind-

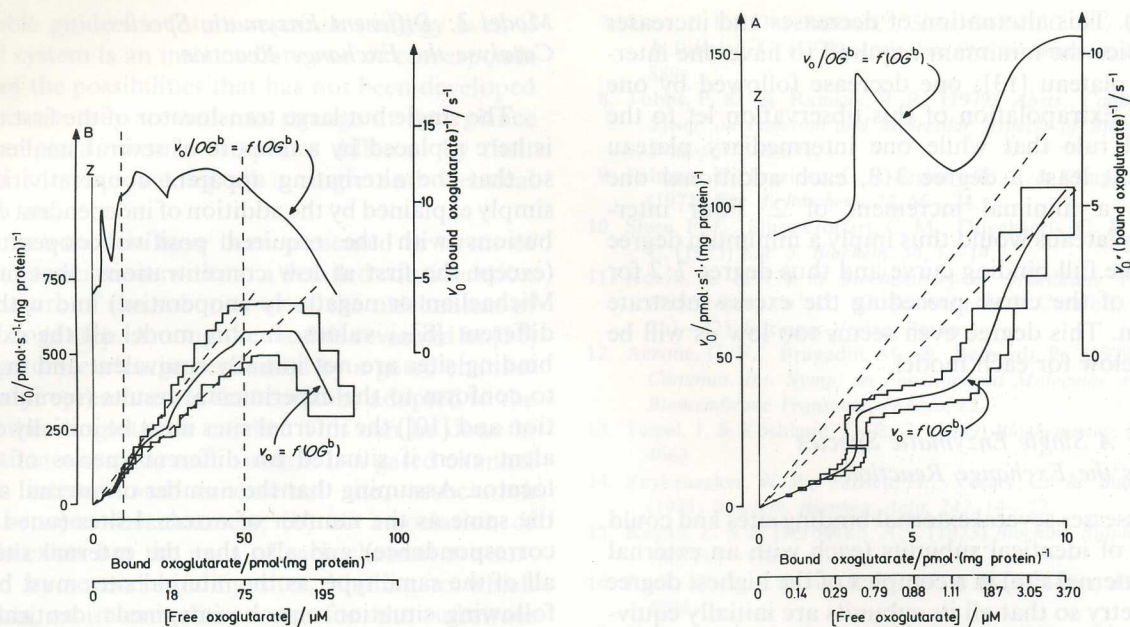


Fig. 8. Initial rate of oxoglutarate uptake at 4-mM internal malate (lower curve) and rate:binding ratio (upper curve) as a function of bound oxoglutarate. The rate and binding values are obtained from the smoothed curves of Fig. 6. The figure shows a succession of rectangles of which the horizontal sides represent the estimated S.E.M. for the binding (9.5%) and the vertical sides represent the estimated standard deviation for the rate of exchange (8% for oxoglutarate concentrations lower than 10 μM , and 15% for oxoglutarate concentrations higher than 10 μM). These uniform estimations were drawn from the distribution of standard errors (or deviations) as a function of binding (or rate). The lower scale (free-oxoglutarate concentrations from 0.05 to 250 μM) is given to facilitate the discussion. The dashed lines are the estimated limits of error of a straight line passing through the origin (drawn from the results obtained between 10 and 50 pmol of oxoglutarate bound per mg of protein) which would correspond to a fixed rate: binding ratio

ing to the translocator would then be a negligible part of the total binding; the extrabinding would be represented by the (horizontal) distance between the Z line and the experimental curve. The binding to the translocator would thus be a very small part of the total binding and this is unreasonable owing to the similarities between the binding and rate curves over such an extended range of oxoglutarate concentrations (Fig. 6).

Since the rate versus specific binding cannot reasonably be a straight line passing through the origin, a single and fixed rate constant for the exchange reaction is not supported by an analysis of the experimental results. It is however the apparent K -effect which is the most striking and imposes the general shape of the kinetic saturation curve up to 50- μM external oxoglutarate.

INTERPRETATION AND CONCLUSION

In order to interpret the complex curves obtained by variation of the external oxoglutarate (four intermediary plateaus in the binding curve, three intermediary plateaus and excess-substrate inhibition in the kinetic-saturation curve) we will consider that

each of them is expressed by the ratio of two polynomials of the oxoglutarate concentration with a numerator degree equal to n and a denominator degree equal to m ($n:m$ degree): see Eqn (1) in [10] and in [19].

At binding-equilibrium conditions, as the oxoglutarate translocator works, m is equal to (or could be less than) the number of associated binding sites if only one translocator species is present. If different non-interconvertible species of translocator are implied, m is equal to the sum of the denominator degree of each species. For the binding equation n must be equal to m while for the kinetic equation n can be less than m (in the case of dead-end substrate inhibition).

General rules for finding the minimum degree of a complex curve, summarized in [19], have been applied. A count of inflexions [33] in the double-reciprocal plot of binding data gives the highest value 5:5 for the minimum degree. We have found that this degree is too low to generate four intermediary plateaus by calculating artificial binding curves with various sets of coefficients in the 5:5 equation. It has not been possible to generate a curve with more than two intermediary plateaus. When two intermediary plateaus appear the intrinsic binding constants are such that $K_1 > K_2 < K_3 > K_4 < K_5$ (K_i is the intrinsic association constant [13] of the substrate to the ES_{i-1}

complex). This alternation of decreases and increases is just twice the minimum required to have one intermediary plateau [13]: one decrease followed by one increase. Extrapolation of this observation led to the empirical rule that while one intermediary plateau requires at least a degree 3:3, each additional one demands a minimal increment of 2. Four intermediary plateaus would thus imply a minimum degree 9:9 for the full binding curve and thus degree 7:7 for the part of the curve preceding the excess-substrate inhibition. This degree even seems too low as will be shown below for each model.

Model 1: A Single Enzymatic Species Catalyses the Exchange Reaction

It possesses several external binding sites and could be made of identical subunits (each with an external and an internal site) in a complex of the highest degree of symmetry so that all its subunits are initially equivalent (a conclusion reached in [10] is that on one side of the membrane at least all the binding sites must be initially equivalent).

The substrate-induced K and V effects observed may be due to conformational changes that principally affect the affinity for the substrate. One point still difficult to understand is how the affinity could alternately decrease and increase as indicated by the existence of intermediary plateaus in the binding curve [13].

The intermediary plateaus represent partial saturations that correspond to complexes with particularly lowered affinity for the substrate. The bound oxoglutarate in each intermediary plateau is approximately proportional to the number of sites in the corresponding complexes. The oxoglutarate binds to the translocator in five saturation steps among which the first four will correspond to catalytic sites. With the minimal number of seven catalytic sites (see above) the expected ratios would be about 1:3:5:7. However as the fourth jump is well characterized and leads to a doubling of the bound oxoglutarate that corresponds to at least five sites it is rather probable that the degree that leads to full saturation of catalytic sites is $\geq 10:10$ (i.e. 2 times 5:5). In fact the observed ratios are approximately 1:3:9:18:27 (the last one corresponds to additional binding that inhibits the exchange reaction), i.e. 2.7:8:24:48:75 pmol of oxoglutarate bound per mg of protein. The high number of associated sites (18) obtained in this way has to be considered with caution and only indicates that the degree is probably higher than 10. The complex with half saturation of catalytic sites seems to have a particular significance as indicated by the rather horizontal plateau that corresponds to it. This could be due to an extensive configuration change favored by the possible high symmetry of this intermediary complex.

Model 2: Different Enzymatic Species Catalyse the Exchange Reaction

The single but large translocator of the first model is here replaced by a mixture of several smaller ones so that the alternating apparent cooperativities are simply explained by the addition of independent contributions with the required positive cooperativities (except the first at low concentrations, that may be Michaelian or negatively cooperative) and with very different $[S]_{0.5}$ values. In this model all the external binding sites are not initially equivalent and in order to conform to the experimental results (see introduction and [10]) the internal sites must be initially equivalent even if situated on different species of translocator. Assuming that the number of internal sites is the same as the number of external sites (one-to-one correspondence) and also that the external sites are all of the same type, as the internal sites must be, the following situation may be imagined: identical subunits are associated in a mixture of multiples (for example, monomer, dimer, trimer, etc.) and are so arranged, in each type of association, as to interact on the external side of the membrane only so that the external sites are modified by various degrees of the subunit association while the internal sites are not. If this model is correct the internal binding sites are not interacting and the apparent positive cooperativity observed in the kinetic-saturation curve by the internal substrate must have another explanation like the two (a and b) proposed in Results and Discussion.

Our saturation curves require at least four species. Retaining the smallest possible one, the following set is obtained: monomer + dimer + trimer + tetramer. The minimum degree of the binding and kinetic equations before the excess-substrate inhibition is thus 10:10 as in model 1. The intermediary plateau at half saturation of the active sites is purely accidental in the scope of this second model while the first model does provide an explanation.

A last remark has to be made: it was assumed at the beginning of this section that the saturation equations are the ratio of two polynomials solely of the substrate concentration; this implies that the association and the dissociation reactions between the different polymers are too slow to be taken into account (this assumption is plausible considering the location in a membrane and the 2°C temperature). If this was not the case the equation of saturation would not be the ratio of two polynomials in the substrate concentration but the ratio of two more complex functions of it [21]. However this last type of equation produces smooth curves even when intermediary plateaus are present in the absence of rapid interconversion of species [20].

The two models proposed are two typical extreme cases that could account for the results. They constitute

a valuable guide for future research strategy even if the real system is an intermediate one or corresponds to one of the possibilities that has not been developed here because they seemed too strange at first glance (for example a mixture of species different by their external sites but having all a single and identical internal site).

The two models have been presented in terms of 'subunit' associations without a detailed consideration of the nature of the subunits or of the mechanism of the exchange step. Among the models reviewed in [34] an obligatory exchange performed by a gated channel is the only representation that could be adapted to the case of the oxoglutarate carrier. This can be done in two distinct ways: (a) each subunit is a gated channel with an internal and an external site; association occurs between the channels; (b) no association of channels exists but the ends of each channel are surrounded by several binding sites, binding to which represents an intermediary step for the substrate between the solution and the channel itself. Model 1 leads to a high, but unique, number of interacting external binding sites; model 2 predicts a smaller number of interacting sites arranged in groups of various sizes.

Whatever the real system is, two additional important features are pointed out: the importance of the apparent K -effect and the high degree (minimum 10:10) of the saturation equations.

This work was made possible by a grant of the *Fonds de la Recherche Scientifique Médicale*. Our thanks are also due to the *Donation Philippe Lefèvre* and to the *Fondation Médicale Mathilde Horlait-Dapsens* for their financial support, to Prof. H. van Cauwenberge for his help, and to G. Espreux for having built the inhibitor-stop equipment. We are grateful to Dr G. Goffart who has helped in devising the numerical treatment of the data. We also wish to thank Dr A. S. Beedle for reading the manuscript and suggesting some changes.

REFERENCES

- Papa, S., Lofrumento, N. E., Quagliariello, E., Meijer, A. J. & Tager, J. M. (1970) *J. Bioenerg.* 1, 287–307.
- Sluse, F. E., Meijer, A. J. & Tager, J. M. (1971) *FEBS Lett.* 18, 149–153.
- Sluse, F. E., Ranson, M. & Liébecq, C. (1972) *Eur. J. Biochem.* 25, 207–217.
- Sluse, F. E., Goffart, G. & Liébecq, C. (1973) *Eur. J. Biochem.* 32, 283–291.
- Sluse, F. E. & Liébecq, C. (1973) *Biochimie (Paris)* 55, 747–757.
- Cleland, W. W. (1963) *Biochim. Biophys. Acta*, 67, 104–137.
- Williamson, J. R., Murphy, E., Coll, K. E. & Viale, R. O. (1979) *Abstr. Commun. Int. Symp. on Function and Molecular Aspects of Biomembrane Transport, Fasano*, 27.
- Sluse, F. E., Duyckaerts, C., Sluse-Goffart, C. M., Fux, J.-P. & Liébecq, C. (1978) *Arch. Int. Physiol. Biochim.* 86, 888–889.
- Tubbs, P. K. & Ramsay, R. R. (1979) *Abstr. Commun. Int. Symp. on Function and Molecular Aspects of Biomembrane Transport, Fasano*, 17.
- Palmieri, F., Prezioso, G., Quagliariello, E. & Klingenberg, M. (1971) *Eur. J. Biochem.* 22, 66–74.
- Sluse, F. E., Sluse-Goffart, C. M., Duyckaerts, C. & Liébecq, C. (1975) *Eur. J. Biochem.* 56, 1–14.
- Kotyk, A. (1977) in *Biochemistry of Membrane Transport, FEBS Symp. n° 42*, (G. Semenza & E. Carafoli, eds) pp. 212–221, Springer-Verlag, Berlin.
- Azzone, G. F., Bragadin, M. & Bernardi, P. (1979) *Abstr. Commun. Int. Symp. on Function and Molecular Aspects of Biomembrane Transport, Fasano*, 15.
- Teipel, J. & Koshland, D. E., Jr (1969) *Biochemistry*, 8, 4656–4663.
- Zeylemacker, W. P., Jansen, H., Veeger, C. & Slater, E. C. (1971) *Biochim. Biophys. Acta*, 242, 14–22.
- Kagan, Z. S. & Doroshko, A. I. (1973) *Biochim. Biophys. Acta*, 302, 110–128.
- Rock, M. G. & Cook, R. A. (1974) *Biochemistry*, 13, 4200–4204.
- Hollander, P. M., Bartfal, T. & Gatt, S. (1975) *Arch. Biochem. Biophys.* 169, 568–576.
- Crabbe, M. J. C. & Bardsley, W. G. (1976) *Biochem. J.* 157, 333–337.
- Bardsley, W. G. & Crabbe, M. J. C. (1976) *Eur. J. Biochem.* 68, 611–619.
- Cook, P. F. & Wedding, R. T. (1978) *J. Biol. Chem.* 253, 7874–7879.
- Wong, J. T.-F. (1975) *Kinetics of Enzyme Mechanisms*, Academic Press, London.
- Sluse, F. E., Sluse-Goffart, C. M., Duyckaerts, C. & Liébecq, C. (1978) *Arch. Int. Physiol. Biochim.* 86, 887–888.
- Sluse, F. E., Duyckaerts, C., Sluse-Goffart, C. M. & Liébecq, C. (1978) *Arch. Int. Physiol. Biochim.* 86, 886–887.
- Sluse, F. E. (1979) *Abstr. Commun. Int. Symp. on Function and Molecular Aspects of Biomembrane Transport, Fasano*, 41.
- Tyler, D. D. & Gonze, J. (1967) *Methods Enzymol.* 10, 75–77.
- Bergmeyer, H. U. & Bernt, E. (1963) in *Methods of Enzymatic Analysis* (Bergmeyer, H. U., ed.) pp. 324–327, Academic Press, New York.
- Hohorst, H. J. & Reim, M. (1963) in *Methods of Enzymatic Analysis* (Bergmeyer, H. U., ed.) pp. 335–339, Academic Press, New York.
- Hohorst, H. J. (1963) in *Methods of Enzymatic Analysis* (Bergmeyer, H. U., ed.) pp. 328–332, Academic Press, New York.
- Meyer, A. J. (1971) *Anion Translocation in Mitochondria*, PhD Thesis, University of Amsterdam.
- von Beisenherz, G., Boltze, H. J., Bücher, T., Czok, R., Garbade, K. H., Meyer-Arendt, E. & Pfeleiderer, G. (1953) *Z. Naturforsch. Teil. B*, 8, 555–577.
- Fux, J.-P., Sluse, F. E., Sluse-Goffart, C. M., Duyckaerts, C. & Liébecq, C. (1979) *Arch. Int. Physiol. Biochim.* 87, 411–412.
- Bardsley, W. G. (1976) *Biochem. J.* 153, 101–117.
- Weidemann, M. J., Erdelt, H. & Klingenberg, M. (1970) *Eur. J. Biochem.* 16, 313–335.
- Bardsley, W. G. & Childs, R. E. (1975) *Biochem. J.* 149, 313–328.
- Deves, R. & Krupka, R. M. (1978) *Biochim. Biophys. Acta*, 513, 156–172.

F. E. Sluse, C. Duyckaerts, and C. Liébecq, Laboratoire de Biochimie et de Physiologie Générales, Institut Supérieur d'Education Physique de l'Université de Liège, Rue des Bonnes-Villes 1, B-4020 Liège, Belgium

C. M. Sluse-Goffart, Département de Chimie Générale et de Chimie Physique, Institut de Chimie, Université de Liège au Sart-Tilman, B-4000 Liège, Belgium